Engineering Structures 132 (2017) 278–287

Contents lists available at ScienceDirect

Engineering Structures

journal homepage: www.elsevier.com/locate/engstruct

Experimental research on the behaviour of concrete-to-concrete interfaces subjected to a combination of shear and bending moment

Eduardo Cavaco [a,*], José Camara [b]

[a] CEris, FCT – Universidade NOVA de Lisboa, Almada, Portugal
[b] CEris, IST – Universidade de Lisboa, Lisboa, Portugal

ARTICLE INFO

Article history:
Received 4 March 2016
Revised 18 October 2016
Accepted 17 November 2016
Available online 25 November 2016

Keywords:
Concrete-to-concrete
Interface
Shear-friction
Precast construction

ABSTRACT

The shear strength of concrete-to-concrete interfaces subjected to either shear or normal forces perpendicular to the interface, or to a combination of both, has been predicted using the "*shear-friction theory*" developed in the 60's for connections for the precast construction. The "*shear-friction theory*" has been developed considering shear failure as pure slippage, and not in combination with a tension crack, and it has been adopted in most design codes worldwide. Although several improvements have been made to the original theory in the last 50 years, few have addressed the behaviour of interfaces subjected to a combination of shear and bending moment, where a shear slippage may occur along a tension crack and a compression zone. This is a relevant issue for the design of both cast-in-place and precast reinforced concrete structures.

This paper, presents an experimental work addressed to the study of the behaviour of concrete-to-concrete interfaces subjected to a combination of shear and bending moment. The influence of the interface on the global behaviour and shear and bending strengths of a beam specimen are addressed, as well as the application of the design expressions.

Results show that the load transfer capacity across the interface is reduced due to the bending moment crack opening, but it has no influence on the shear and the bending strengths of the beam specimen. However, the bending ductility of the latter is partially reduced due to a shear slippage occurred after the formation of a plastic hinge, and the collapse of the compression zone. It was not possible to evaluate the accuracy of the design expressions to predict the interface maximum friction strength. However, the general application of these expressions to this situation is doubtful, as they are incapable to predict the strength deterioration occurred after the yielding of the longitudinal reinforcement.

1. Introduction

On reinforced concrete structures, load transfer across concrete-to-concrete interfaces needs to be considered when two concretes are cast against each other at different times, and the hardening process of the older concrete is already finished. For cast-in-place structures, concrete-to-concrete interfaces are a natural result of the building process when a single concrete casting is not possible, due to limited production resources or due to unforeseen events leading to interruptions in the erection process. Concrete-to-concrete interfaces may also result from the connection of precast to cast-in-place elements and from the strengthening and/or repairing works, on existing structures, when new concrete layers are added to the existing structural elements (slabs, beams and columns) to enlarge original sections. At design stages, and when possible, construction joints are usually foreseen to sections where internal forces and stresses are reduced. However, this is not always possible and concrete-to-concrete interfaces may also be found at more force demanding sections. Especially in these cases, an adequate understanding of the interface behaviour is required due to the eventual impact on the structural safety.

The behaviour of concrete-to-concrete interfaces subjected to shear or normal forces perpendicular to the interface, or a combination of both, where a shear slippage is possible to occur, is relatively well studied, having been the object of several research works published in the latter 50 years. The "*shear-friction theory*", originally proposed by Birkeland and Birkeland [2], has been used to predict the shear strength of concrete interfaces. It has seen major improvements over the years, as a result of several research works, and it has been adopted in most design codes. The application of code expressions to the design of concrete-to-concrete interfaces loaded by shear or normal forces or a combination of both does not raise significant doubts. However, when a combination of shear

* Corresponding author.
E-mail address: e.cavaco@fct.unl.pt (E. Cavaco).

http://dx.doi.org/10.1016/j.engstruct.2016.11.041
0141-0296/

Notation

α	angle between shear reinforcement and the shear plane
β	coefficient allowing for angle of concrete diagonal strut
c	coefficient of cohesion
f_c	concrete compressive strength
f_{cm}	mean value of concrete compressive strength
f_{ctd}	design value of concrete tensile strength
f_{ctm}	mean value of concrete tensile strength
f_y	yield strength of reinforcement
f_{ym}	mean value of yield strength of reinforcement
k_1	Randl's coefficient of efficiency of reinforcement
k_2	Randl's dowel action coefficient
μ	coefficient of friction
v	strength reduction factor
v_u	ultimate shear friction strength
ρ	reinforcement ratio
σ_n	normal stress acting on interface due to external loading
A_{sl}^-	negative longitudinal reinforcement area
A_{sl}^+	positive longitudinal reinforcement area
A_{sw}	transversal reinforcement area
M_{max}^-	maximum negative bending moment
M_{max}^+	maximum positive bending moment
M_{Rm}	bending strength
P_{Rm}^M	expected ultimate testing load due to a bending failure
P_{Rm}^S	expected ultimate testing load due to a shear friction failure
P_{Rm}^V	expected ultimate testing load due to a shear failure
V_{Rm}^M	shear load at the time of a bending failure
V_{Rm}^S	shear friction strength
V_{Rm}^V	shear strength

force and bending moment is considered, the application of the same expressions to check the interface safety seems at least questionable, since the "*shear-friction theory*" has been developed having in mind the shear failure as slippage along a plane of maximum shear, and not as part of a tension crack, in the usual sense [2]. In other words, and using the terminology of the mechanics of fracture, the theory addresses the shear slippage along mode II but not along mode I. Moreover, the issue has not often been addressed in the improvements made to the original "*shear-friction theory*" and rarely has been discussed on the published research works. However, it stays clear in the codes that shear transfer across interfaces between two differently aged concretes, even where a flexion tension crack is likely to develop, e.g. corbels, needs to be considered. Since the behaviour, in terms of strength and ductility, of interfaces under these conditions is not well known, further research is still needed.

2. Literature review

2.1. "Shear-friction theory"

The load transfer mechanism of shear forces between the interface defined by two differently aged concretes has been predicted using the "*shear-friction theory*", originally proposed by Birkeland and Birkeland [2], developed in response to the design of connections for the precast concrete construction. The working principle of the original theory is usually depicted with a "*saw-tooth model*" and it is based on the following hypothesis: slippage at shear joint results in the opening of the joint, which generates tensile forces in any reinforcement bars crossing the interface. By equilibrium, compressive stresses tend to develop at the interface, generating friction according to the surface roughness. The ultimate shear stress at the concrete-to-concrete interface is given by Eq. (1) which, according to Birkeland and Birkeland [2] is not meant to be applied to shear interfaces associated with corbels, bearing shoes, ledger beam bearings and the like. Concrete-to-concrete (or concrete-to-steel) interfaces, as well as potential cracks in monolithic concrete, ordinary beam shear-flexure and principal tension analyses are also not covered by the "*shear-friction theory*" [2].

$$v_u = \mu \rho f_y \tag{1}$$

Since the first proposal of the "*shear-friction theory*", several modifications have been suggested in order to improve its accuracy and to take into account the effects of adhesion, aggregate interlock, dowel action and the weakest concrete. Many research papers, including experimental and numerical studies, can be found in the literature. An exhaustive revision of the subject is presented in Santos and Júlio [10]. The most important milestones there highlighted are:

- the "*modified shear-friction theory*" proposed by Mattock and Hawkins [5] which suggested the addition of a second term to Eq. (1) related to cohesion and the complementary effect of external clamping stresses that increase friction at the interface;
- the "*sphere-model*" proposed by Walraven et al. [16] that takes into account, in a more consistent form, the interaction between aggregates, the binding paste and the interface zone;
- the research of Tassios and Vintzēleou [11] and Tsoukantas and Tassios [12] on the influence of the dowel action mechanism in the ultimate shear strength of the interface;
- the work of Randl [7], the "*extended shear-friction theory*", proposing, in a single equation, Eq. (2), the contribution of three different load transfer mechanisms: (i) cohesion, due to aggregate interlocking and the adhesion between differently aged concretes; (ii) friction, resulting from stresses perpendicular to the interface and slippage, thus depending on the crossing reinforcement, clamping stresses and surface roughness; and finally (iii) dowel action, due to flexural resistance of reinforcement bars sewing the interface. The latter has been adopted by the very recent Model Code 2010 [17].

$$v_u = c f_c^{1/3} + \mu(\rho k_1 f_y + \sigma_n) + k_2 \rho \sqrt{f_y f_c} \leqslant \beta v f_c \tag{2}$$

2.2. Design expressions

The research mentioned above has been the basis of the design expressions adopted in all design codes. According to ACI 318-14 [1] shear transfer across any given plane, such as an existing or potential crack, an interface between different materials or an interface between two concretes cast at different times, should be evaluated for possible failure by shear slippage. The ultimate shear strength is given by Eq. (3), which does not account directly with cohesion and dowel action.

$$v_u = \rho f_y(\mu \sin\alpha + \cos\alpha) \tag{3}$$

The expression proposed by the Eurocode 2 [3] is given in Eq. (4). It is similar to the proposal of Randl [7], but it does not explicitly considers the dowel action contribution.

$$v_u = cf_{ctd} + \mu\sigma_n + \rho f_y(\mu \sin\alpha + \cos\alpha) \leqslant 0.5vf_c \quad (4)$$

Beyond the contribution of cohesion, the major difference between both design expressions lies in the classification of the surface roughness, carried out qualitatively. Due to the impact on the ultimate shear strength, recent research has been produced and new quantitative methods have been suggested to assess the roughness of the surface [9].

2.3. Eccentricity effect

The "*shear-friction theory*" was developed having in mind connections in precast construction where shear failure as slippage, and not as part of a tension crack, is likely to occur. On the following improvements made, effects of shear eccentricity and the presence of bending moment at the interface, haven't been addressed often. The majority of experimental tests, giving support to the produced research, have been carried out using push-off specimens with null eccentricity. Due to the recognized influence of the latter, special specimens have been produced to eliminate accidental eccentricity of traditional push-off specimens [8].

The research work of Mattock et al. [6] is one of the few found testing the application of the "*shear-friction theory*" to evaluate shear load transference in concrete-to-concrete interfaces subjected to both shear and bending moments. A corbel type push-off specimen has been used and different eccentricities for the applied load and different reinforcement arrangements have been tested. Results of the experimental campaign show that the ultimate shear which can be transferred across a crack is not significantly affected by the presence of a moment in the crack, providing the applied moment is less than or equal to the flexural capacity of the cracked section. Design recommendations are also provided in this study that include the arrangement of the longitudinal reinforcement, preferentially located in the flexural tension zone, in order to maximize the joint strength to slippage.

Although, the effect of the bending moment is not addressed in the Eurocode 2 [3], a reference is made in the ACI 318-14 [1], based on the research work carried out by Mattock et al. [6]. It is referred that where a moment acts on a shear plane, the flexural compression and tension forces are in equilibrium and do not change the resultant compression acting across the shear plane. It is further stressed in the ACI 318-14 that is not necessary to provide additional reinforcement to resist the flexural tension stresses, unless the required flexural tension reinforcement exceeds the amount of shear-transfer reinforcement provided in the flexural tension zone.

Therefore, the longitudinal reinforcement can serve simultaneously the two purposes and no interaction between moment and shear load transference has to be considered. However, it has to be stated that the application of the "*shear-friction theory*" to a concrete-to-concrete interface subjected to a combination of shear and bending moment is doubtful, since the original theory does not explicitly cover this case, and insufficient research on the subject still exists. The original theory is based on the hypothesis that friction is the basic strength mechanism activated by clamping stresses, resulting either from external compression forces or from the equilibrium with the tensile forces developed in the reinforcement bars, caused by the separation of the interface, due to the slippage and the roughness of the surfaces in contact. It is also supposed that both the compression and tensile stresses are in equilibrium in the same place of the interface, which is not the case when considering a tension crack resulting from a bending moment. In this case, the interface is subjected to stress and deformation gradients. The interface opening results from the elongation of steel bars due to the bending tensile stresses, rather than from the slippage of the rough surfaces in contact. In this manner, it is believed that an interaction between the shear friction strength and the acting bending moment exists, due to limited capacity of the compressed zone to transfer shear stresses and the potential degradation of the friction mechanism in the tensile zone due to the crack opening.

Moreover, very few tests have been made and important aspects such as the cross section shape, or the impact on the section ductility, have never been discussed.

3. Experimental research

The experimental work described in this paper was planned to: (a) analyse the application of the design expressions, based on the "*shear-friction theory*", to evaluate the shear load transfer across an interface between two differently aged concretes, when simultaneously subjected to a bending moment; (b) investigate the effect of a concrete-to-concrete interface on the ultimate shear and bending strengths of a beam cross section; (c) and to check the impact of a shear joint in the bending ductility of a beam cross section.

Tested specimens consisted on four "I" beams with 5.0 m length and 0.50 m height, loaded at one section and supported at three points to simulate the lateral span of a continuous beam with 3.0 m length (see Fig. 1). The left short span was created to allow negative bending moments to develop over the continuous support. It was over reinforced in order not to influence the behaviour of the main span. The loaded section was defined closer to the simple support, on the right end, in order to have identical shear forces on both supports.

The four beams were divided into two sets. The first set, with the reference V_1, aimed mainly at investigating the influence of the concrete-to-concrete interface on the ultimate shear capacity. The second set, with the reference V_2, has been designed for the study of the interface effect on the flexural behaviour (ultimate strength and ductility). Two beams, one of each set, were built on a single concrete cast with no shear joints. These beams (V_{1Ref} and V_{2Ref}) served as reference. The remaining specimens (V_{1P} and V_{2P}) were casted in two stages as shown in Figs. 1 and 2, with two interfaces per specimen between differently aged concretes. These interfaces, A and B, were at a distance of 0.25 m of each support, positioned on the hogging and sagging regions, respectively. Preceding the second cast, the hardened concrete surfaces were intentionally scarified with an air impact hammer with the goal of exposing the coarse aggregate and achieving a minimum mean roughness of 3 mm. However a quantitative measure of the interface mean roughness was not carried out, and the interfaces were classified as "rough", according to Eurocode 2 [3] (see Fig. 2).

The longitudinal reinforcement to resist the bending moments of specimens V_1 was overdesigned in relation to the shear reinforcement on the beams web, in order to encourage a shear failure. The opposite was defined for specimens V_2, where a bending failure was enforced by overdesigning the shear reinforcement.

For these specimens, the longitudinal reinforcement crossing the interfaces A and B was almost strictly the necessary to resist the bending tension forces. As suggested by the ACI 318-14 [1], this reinforcement can be used simultaneously for bending and shear friction purposes, without interaction between both. In this case, 4∅6 mm steel bars were adopted in the compression zone, to allow the reinforcement assemblage during the construction stage. Fig. 3 shows the reinforcement detailing of specimens V_1. That of V_2 beams is identical excepting for the web reinforcement where ∅8 mm bars have been used spaced 7.5 cm. For all the specimens both transverse and longitudinal reinforcement have been overdesigned on the short span on the left side of the central support.

Three samples of each steel bar size and three concrete specimens per casting were tested for the tensile yielding strength and the compressive strength, respectively. Concrete tensile

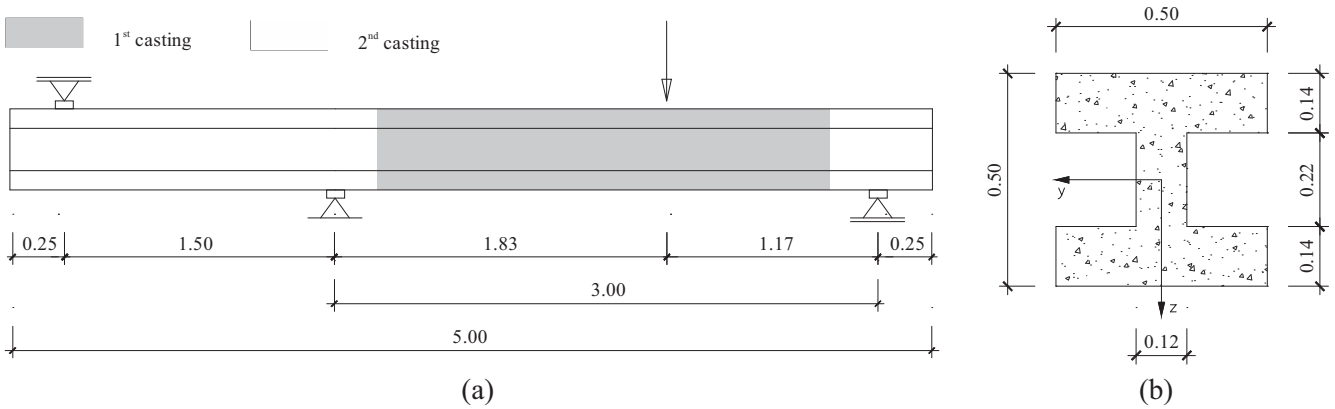

Fig. 1. Beam specimen: (a) side view; (b) cross section.

Fig. 2. Specimens production: (a) precasting stage of specimens $V_{1,P}$ and $V_{2,P}$; (b) before surface preparation; (c) after scarifying and exposing the coarse aggregate.

strength was estimated based on the Eurocode 2 [3]. The mean values of the concrete compressive and tensile strength are presented in Table 1. The second cast of specimens V_{1P} and V_{2P} was executed 15 days after the first one.

Table 2 summarizes the bending strength of specimens assessed using mean values for both steel and concrete strength and according to Eurocode 2 [3]. The ultimate load, determined by a bending failure for a load of 780 kN, corresponds to a shear force crossing the interfaces A and B of 390 kN.

Table 3 summarizes the specimens shear strength controlled by the failure of the stirrups in the web or the concrete crushing at the compression struts, computed according to the Eurocode 2. In the

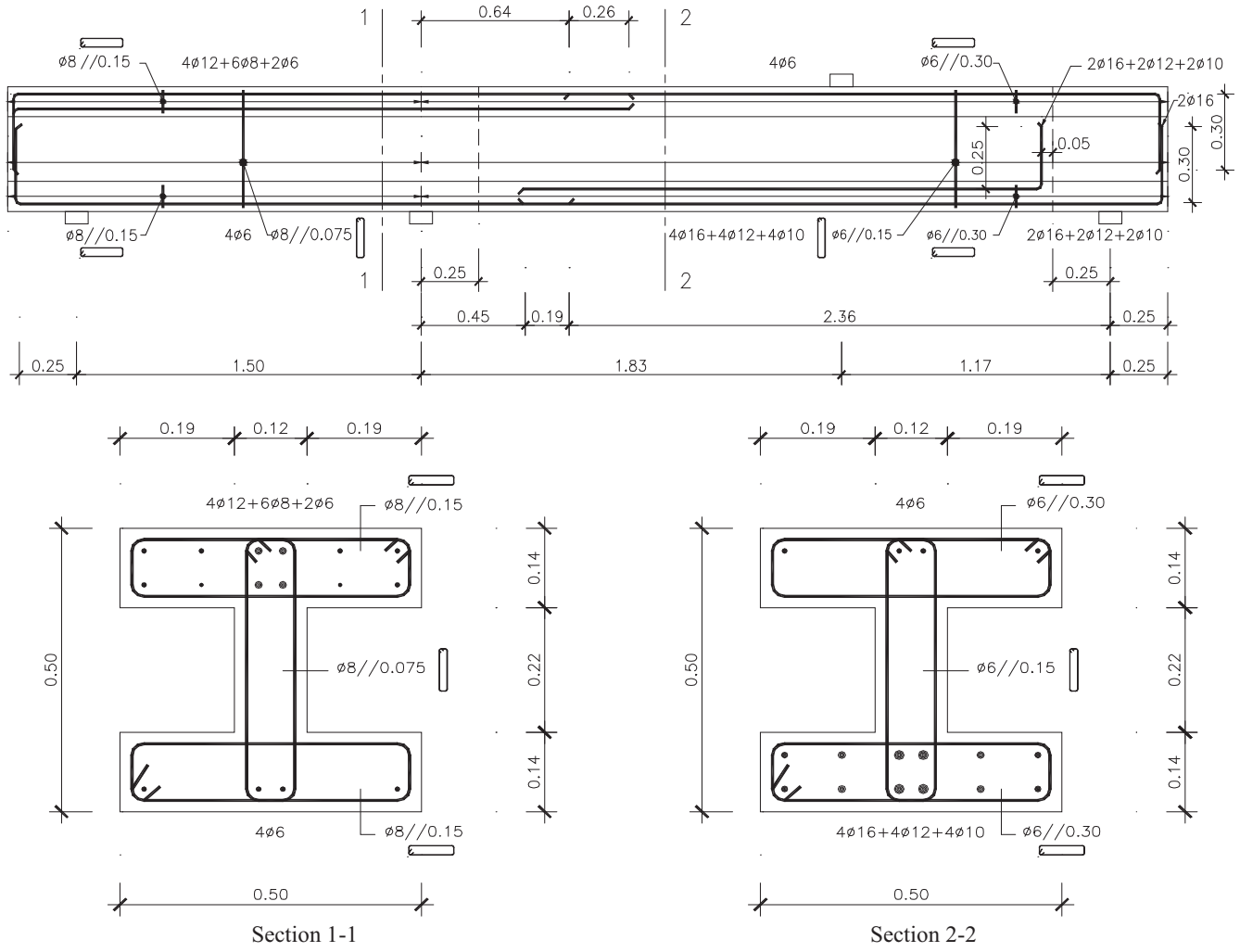

Fig. 3. Reinforcement detailing of specimens V_1.

Table 1
Mean values of the concrete compressive and tensile strengths tested at the 28 days.

Specimen	f_{cm} (MPa)		f_{ctm} (MPa)	
	1st casting	2nd casting	1st casting	2nd casting
V_{1Ref}	30.5		2.39	
V_{2Ref}	31.2		2.44	
V_{1P}	30.0	28.2	2.36	2.22
V_{2P}	38.0	29.5	2.90	2.32

Table 2
Bending reinforcement of specimens and estimated strength.

Section	A_{sl}^{-} (cm^2)	A_{sl}^{+} (cm^2)	f_{ym} (MPa)	M_{Rm} (kN m)	V_{Rm}^{M}/P_{Rm}^{M} (kN)
M_{max}^{-}	8.1	1.1	579	223	390/780
Interface A	8.1	1.1		223	
M_{max}^{+}	1.1	15.7		414	
Interface B	1.1	7.9		216	

Table 3
Shear reinforcement of specimens and estimated strength.

Specimen	A_{sw} (cm^2/m)	V_{Rm}^{V} (kN)	P_{Rm}^{V} (kN)
V_1	3.77	194	388
V_2	13.70	491[a]	982

[a] Crushing at the compression struts.

first case, and based on a developed strut-tie model, an angle of 34° was considered for the failure surface. An approach for the minimum shear strength for compression struts crushing was computed assuming $\mathrm{Cotg}(\theta) = 2$, which corresponds to an angle of 26.5°. The corresponding testing load was 388 kN and 982 kN for specimens V_1 and V_2, respectively.

Table 4 the estimated shear-friction resistance, of the specimens casted in two times, is presented, according to Eqs. (2)–(4). The weakest concrete was considered in the calculations and the equation coefficients were estimated based on the respective codes and on the work of Randl [8]. The reinforcement ratio was assessed using the total amount of reinforcement and the overall cross section area. It is assumed at this stage that no interaction between the bending moment and the shear friction mechanism exists and that a potential failure will include a slippage across both the flanges and the web of the section. This hypothesis is questionable since shear forces usually run through the web of the section. However, it is believed that in order to have a shear friction failure, a full slippage of the entire section is required. Under these conditions, the ultimate testing load, corresponding to a shear slippage along the interface, ranges from 1040 kN to 1132 kN, to specimen V_{1P}, and from 1040 kN to 1142 kN to specimen V_{2P}. Therefore, no significant differences exist between the strength predictions of the different expressions, assuming no interaction with the bending moment.

Table 4
Estimated shear friction strength.

Expression	Specimen	c	μ	k_1	k_2	α (°)	f_{cm}^{min} (MPa)	f_{ctm}^{min} (MPa)	f_{ym} (MPa)	Interface	ρ (%)	V_{Rm}^{S} (kN)	P_{Rm}^{S} (kN)
MC 2010 Eq. (2)	V_{1P}	0.4	1.0	0.5	0.9	–	28.2	2.22	579	A	0.56	580	1132
										B	0.54	566	
	V_{2P}						29.5	2.32		A	0.56	585	1142
										B	0.54	571	
ACI 318 Eq. (3)	V_{1P}	–	1.0	–	–	90	28.2	2.22	579	A	0.56	540	1040
										B	0.54	520	
	V_{2P}						29.5	2.32		A	0.56	540	1040
										B	0.54	520	
Eurocode 2 Eq. (4)	V_{1P}	0.45	0.7	–	–	90	28.2	2.22	579	A	0.56	544	1060
										B	0.54	530	
	V_{2P}						29.5	2.32		A	0.56	551	1076
										B	0.54	538	

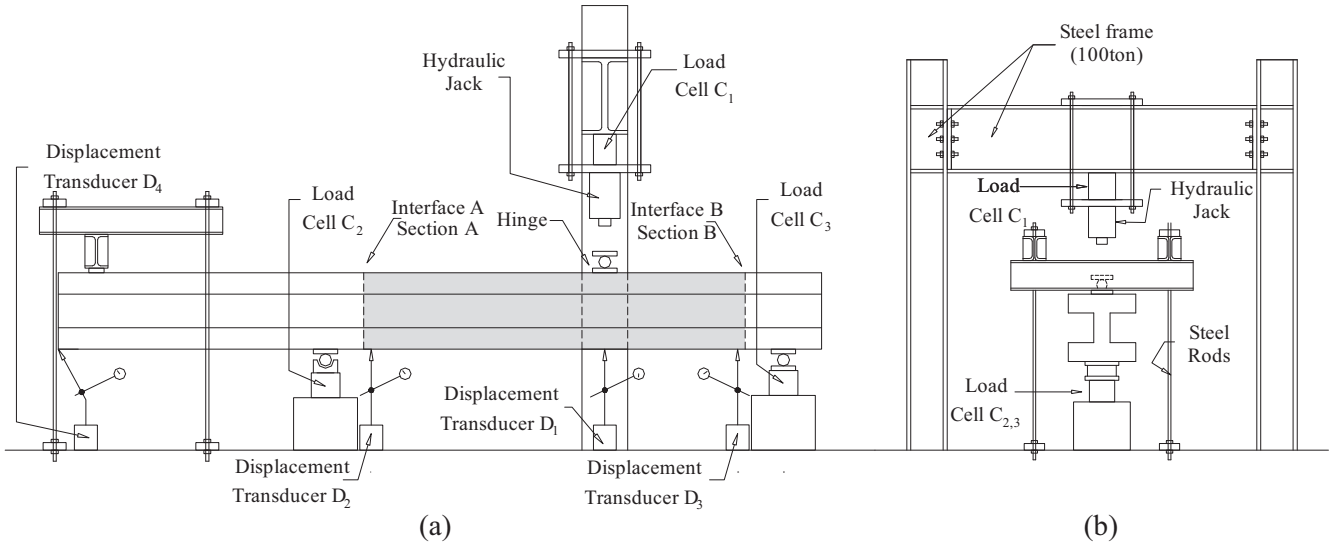

Fig. 4. Experimental setup: (a) side view; (b) front view.

The specimen tests were performed controlling imposed displacement and using a 100 ton hydraulic jack attached to a reaction steel frame with a maximum capacity of 100 ton. Three load cells were used, at the loading section (C_1), at the continuous support (C_2) and at the roller support (C_3). Displacement transducers were at the loading section (D_1), under interfaces A (D_2) and B (D_3) and at end of the shorter span (D_4) to control deformability of the tying system. 10 strain gages per interface (20 per specimen) were used. 5 strain gages were attached to the longitudinal bars exactly at the interface section, and the 5 remaining were distributed by the shear bars on both sides of the casting plane. The reference specimens were instrumented exactly at the same locations of the precasted specimens, and the sections corresponding to interfaces A and B were denoted as sections A and B, respectively. A scheme of the experimental setup is depicted in Fig. 4. The loading protocol included an unloading stage defined for approximately 50% of the expected yielding load of the specimen, simultaneously to simulate a service situation and to check the inexistence of gaps on the bar system attached to the laboratory strong floor.

4. Results

4.1. Specimens V_{1Ref} and V_{1P}

Fig. 5 shows the load displacement diagram obtained for specimens V_{1Ref} and V_{1P}. Identical global behaviour, in terms of stiffness and strength, is observed. The ultimate load of V_{1Ref} was 445 kN that is practically equal to that of specimen V_{1P} of 455 kN.

Fig. 6 shows the same diagonal shear failure mode observed for both specimens due to transverse reinforcement failure on the beam's web. In both cases, failure occurred between the continuous support and the section where the load was applied, defining an angle of 24° with the horizontal plane, thus below the assumptions of the calculation presented in Table 3.

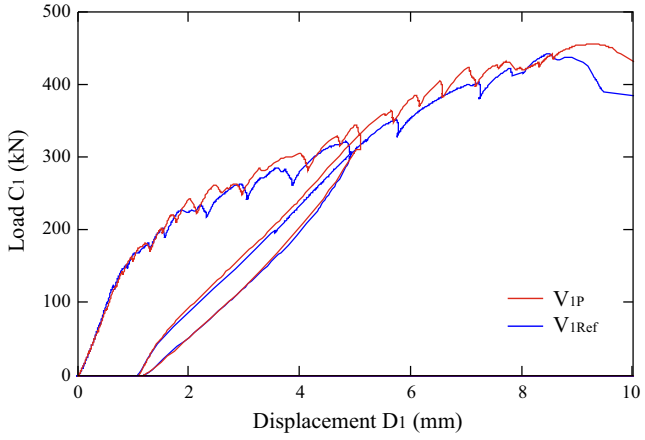

Fig. 5. Load displacement diagram of specimens V_{1Ref} and V_{1P}.

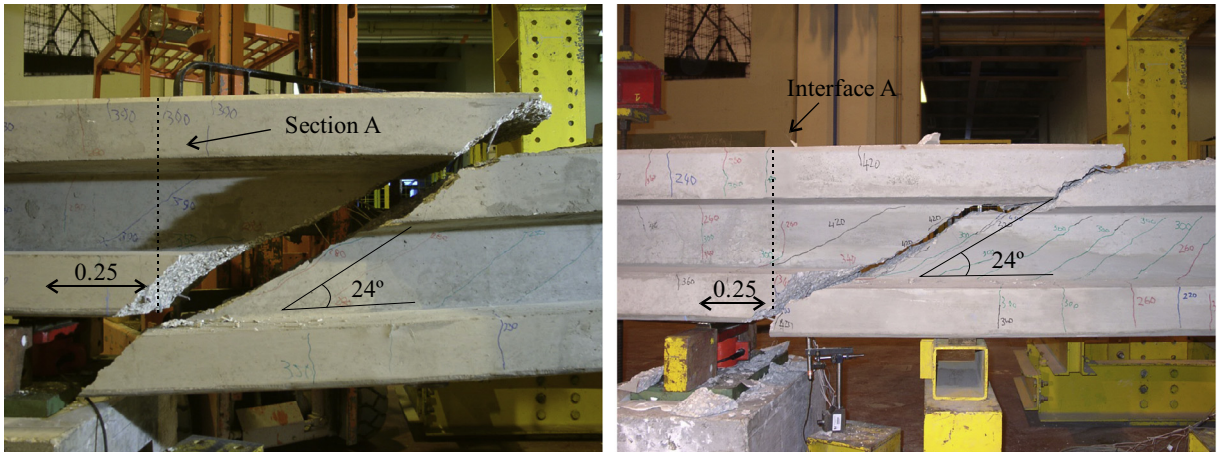

Fig. 6. Failure mode of specimens: (a) V_{1Ref}; (b) V_{1P}.

Ultimate loads were above the estimated value for diagonal shear failure (388 kN see Table 3) since the failure surfaces angles were smaller, in relation to the ones adopted in the former calculations, thus crossing more stirrups.

The casting interfaces, A and B, have had no influence on the global shear behaviour of specimen V_{1P} in comparison to V_{1Ref}. However, V_{1P} presented a variation in the traditional cracking pattern in interface A region, since there were no diagonal cracks crossing the interface, as depicted in Fig. 6(b). On the hogging region, the first vertical crack was observed at interface A, for a testing load of 180 kN, while cracking in the section of maximum negative bending moment, occurred for an imposed load of 240 kN. Since the weakest concrete was from the second casting, which included the continuous support region, it may be admitted that the tensile strength of the concrete-to-concrete interface to be below that of weakest concrete (2.2 MPa, see Table 1). The tensile strength of the interface A, located at the hogging region, was estimated in 1.1 MPa, considering the maximum normal stress from the acting bending moment at cracking. Cracking along interface B, located at the sagging region, occurred for an imposed load of 250 kN and the interface tensile strength was estimated to be 1.7 MPa, therefore also below that of the weakest concrete. It is believed that the difference between the tensile strength of interface A and B can be explained by bleeding of concrete during casting, resulting in a weaker concrete on the upper part of the casted element. The bleeding effect have been investigated by several authors and strength variations of more than 30%, between the upper and lower levels of the structure, have already been reported [4].

Fig. 7 shows the strain records of the longitudinal reinforcement on the interfaces sections of the specimen V_{1P} and the corresponding sections of the specimen V_{1Ref}.

The premature cracking of interface A of specimen V_{1P} is depicted by a sudden strain increase for a testing load of 120 kN, which was visible when the loading force was 180 kN. Cracking of the corresponding section of specimen V_{1Ref} occurred for a testing load of 280 kN. A distinct behaviour was observed in interface B since no significant differences exist between strain records of both specimens. Fig. 6(b) also shows that the premature cracking along interface A changed the expected shear cracking pattern on the beam's web, since no diagonal cracks were observed to cross the interface towards the support, as referred before. The same did not occur in interface B. Table 2 summarizes the main results of the loading tests performed on specimens V_{1Ref} and V_{1P}.

4.2. Specimens V_{2Ref} and V_{2P}

Fig. 8 shows the load displacement diagram obtained for specimens V_{2Ref} and V_{2P}. Both present very similar global behaviour

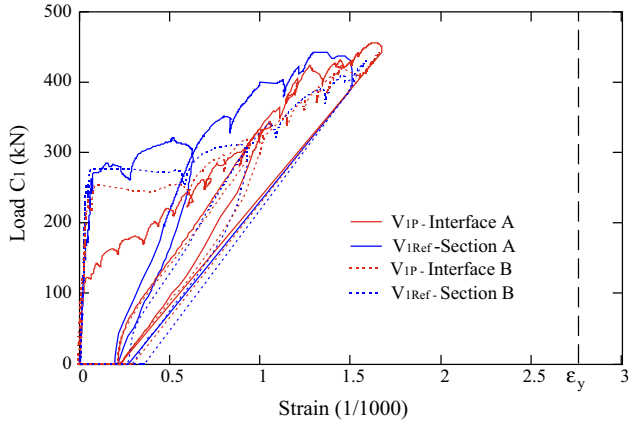

Fig. 7. Strain records of the longitudinal reinforcement at interfaces and sections A and B, for specimen V_{1P} and V_{1Ref}, respectively.

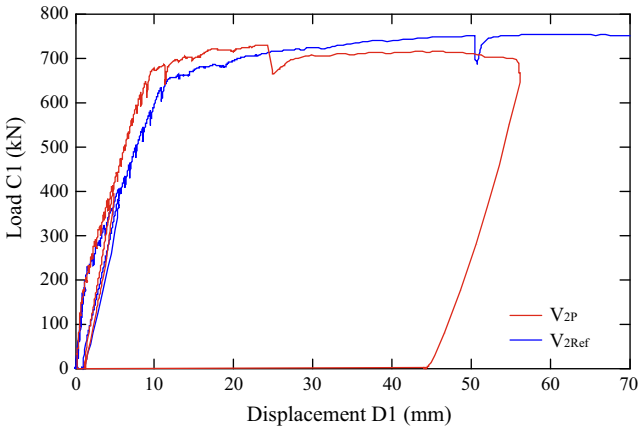

Fig. 8. Load displacement diagram of specimens V_{2Ref} and V_{2P}.

regarding stiffness and strength. Maximum testing loads were 753 kN and 720 kN for V_{2Ref} and V_{2P}, respectively. However, the latter presented significant less plastic deformations, considering that Fig. 8 does not show the maximum vertical displacement of specimen V_{2Ref} (equal to 150 mm), due to the transducer limitations. Moreover, the strain-hardening effect of the failure mechanism was not observed on specimen V_{2P} and the load at the failure, 700 kN, was below the maximum recorded of 720 kN.

Fig. 9 shows the strain records of the longitudinal reinforcement at interfaces A and B for both specimens. Again, early cracking of interface A was observed in relation to section A of specimen V_{2P}. On the other hand, cracking of interface B and of section B of specimen V_{2P} and V_{2Ref}, respectively, occurred for similar testing loads.

Fig. 10 shows the cracking pattern for specimen V_{2P} in the Interface A and B regions. In the first case, the existence of a contact surface weaker in tension resulted in the early and pronounced cracking along the interface, which led to a variation of the diagonal cracking pattern on the beam's web. Fig. 10(a) shows, at interface A, the diagonal cracks in the web being interrupted, due to the reduction of the friction capacity of the interface to transfer shear loads. The opposite was found in interface B, as the traditional diagonal cracking pattern did not suffer variations (see Fig. 10(b)).

Although the global behaviour of both specimens seemed similar, the failure mechanism was not the same, as shown in Fig. 11. The reference beam collapsed after an imposed displacement of 150 mm due to concrete crushing in the top flange bellow the point where the load was applied (see Fig. 11(b)). Earlier, two plastic hinges had been formed, firstly in the sagging region and then in the hogging region (see Fig. 11(a)). The specimen V_{2P} collapsed after the formation of the two hinges, however for an imposed displacement of 55 mm. The plastic stage was interrupted by a sudden shear slippage along interface A, as shown Fig. 11(c). The interface A allowed the plastic hinge development, but limited the plastic strains. Fig. 11(c) and (d) shows that the shear slippage occurred mainly in the top flange and in the web. On the bottom flange, a tension crack developed towards the support, at failure.

Table 6 summarizes results of specimens V_{2Ref} and V_{2P}.

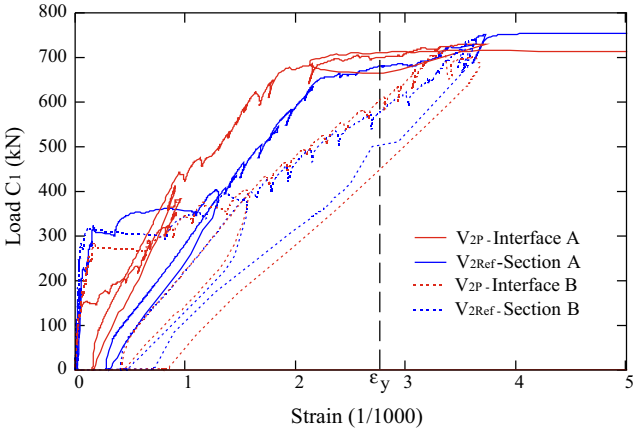

Fig. 9. Strain records of the longitudinal reinforcement at interfaces and sections A and B, for specimen V_{2P} and V_{2Ref}, respectively.

5. Discussion

The early cracking of interface A of specimens V_{1P} and V_{2P}, and the modification of the classical diagonal cracking pattern on the beam's web, indicates that the ability of the interface to transfer shear was reduced, but to the point that had no significant impact on the ultimate shear and bending strengths of both specimens. However, some influence on service limit states may eventually be expected, regarding that cracking of interface A was detected before the section of maximum negative bending moment, and for a testing load compatible with service loads.

The interface friction strength was observed to be variable depending on the crack width opening as the failure occurred for constant shear forces. As suggested by Walraven [15], the capacity to transfer shear stresses across an interface between two differently aged concretes, based on the aggregate interlock mechanism, decreases with the opening of the interface. The same was reported by Vintzēleou and Tassios [14] in relation to the dowel action mechanism. These two hypothesis can explain the fact that the shear slippage occurred during the plastic stage, after the application of the maximum testing load and for constant shear force. Since the interface A was located in the plastic hinge region, after the yielding of the longitudinal reinforcement (see Fig. 9(a)), crack width along the interface increased significantly leading to a deterioration of the shear friction capacity. Shear stresses were then preferentially transferred through the compressed flange up to its failure due to a tension crack. Fig. 12 shows the strain measurements in the first stirrup localized between the interface and the support and in the corresponding stirrup of specimen V_{2Ref}. The latter does not reach the yielding strain, however the first one exceeds it after the maximum load has been reached due to the tension crack developed in the bottom flange. In the research of Vintzēleou and Tassios [13] a similar failure mode in the bottom flange has been documented. For heavily compressed concrete-to-concrete interfaces, the shear slippage was anticipated by the development of a tension crack in the cement matrix.

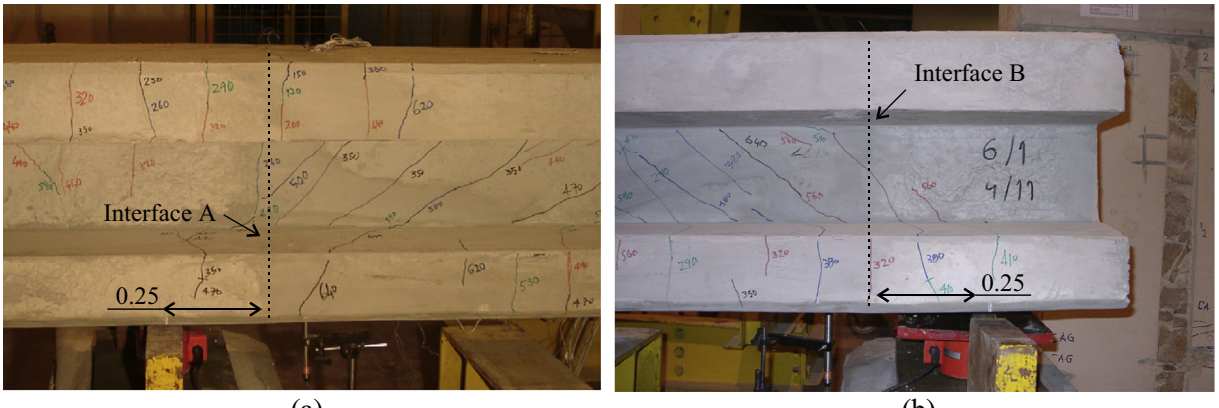

Fig. 10. Cracking pattern of specimen V_{2P}: (a) interface A; (b) interface B.

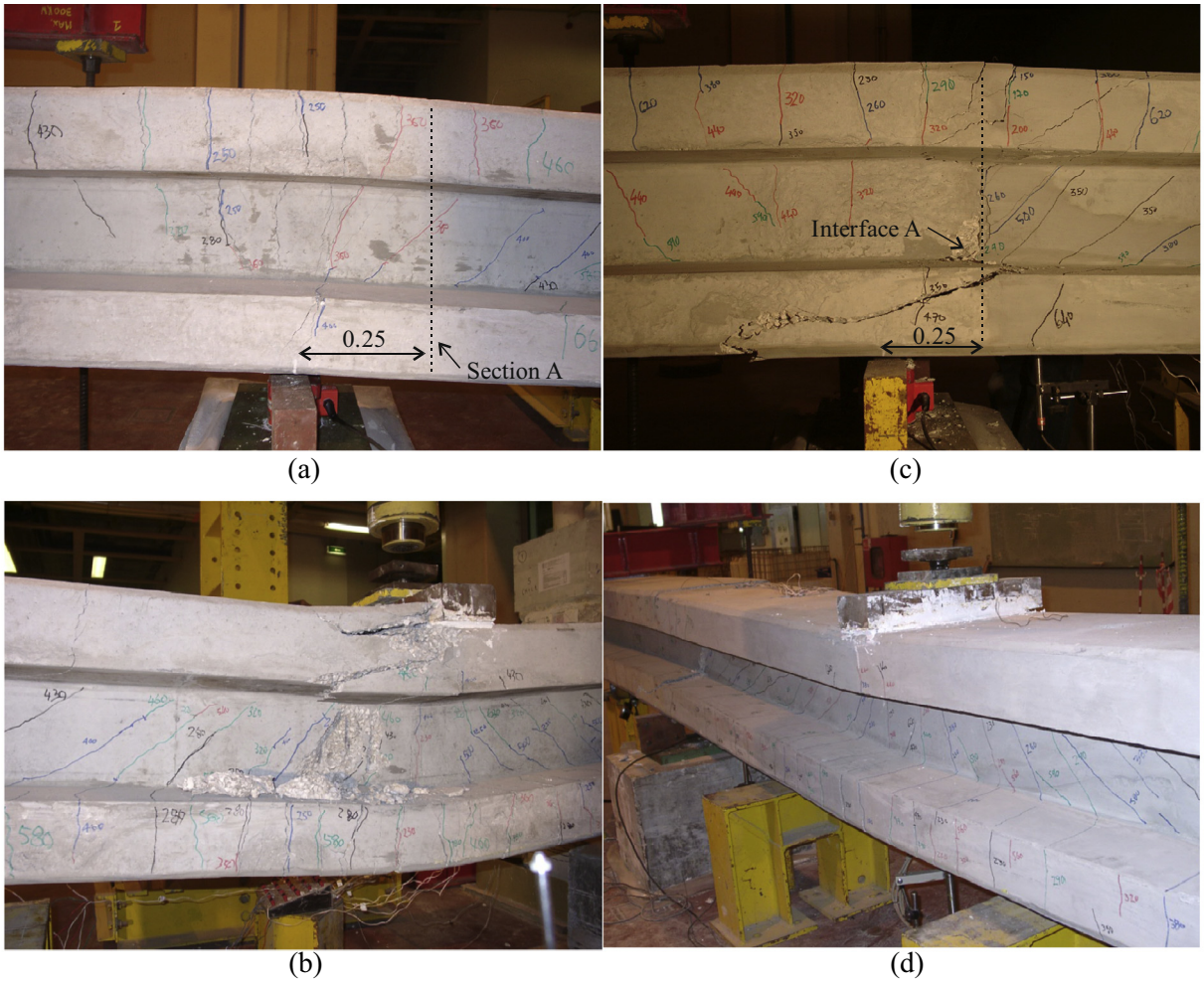

Fig. 11. Failure mechanism of specimens: (a) V_{2Ref} – section A; (a) V_{2Ref} – mid span; (c) V_{2P} – interface A; (d) V_{2P} – mid span.

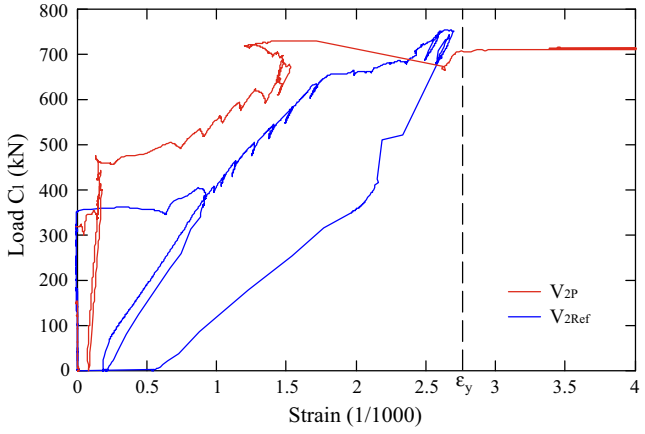

Fig. 12. Strain records of the transverse reinforcement: first stirrup on the left side of interface A of specimen V_{2P}; and corresponding stirrup of specimen V_{2Ref}.

Although additional research is still needed, the application of the design expressions to predict the strength to slippage of an interface subject to pure shear does not seem adequate in the presence of shear and bending moment, as they do not take into account the strength degradation after the formation of a plastic hinge. Moreover, the observed failure mode is not consistent with the theory for pure shear, since it consists of a combination of slippage in the tension zone and the formation of a tension crack in the compressed flange. It is also impractical to distinguish between tension and compressed zones as these are not constant due to the ascending bending moment and due to the stress gradients inside each zone.

Finally, the accuracy of the design expressions to predict the maximum friction strength, prior to the formation of a plastic hinge, could not be evaluated during these tests, as the maximum shear force crossing the interface was always below the estimations (see Tables 4–6).

Table 5
Loading test results of specimens V_{1Ref} and V_{1P}.

Specimen	Cracking in the section of				Ultimate load (kN)	Failure mode
	M^{+}_{max} (kN)	M^{-}_{max} (kN)	Int. A (kN)	Int. B (kN)		
V_{1Ref}	180	200	320	280	445	Shear ($\theta = 24°$)
V_{1P}	160	240	180	250	455	Shear ($\theta = 24°$)

Table 6
Loading test results of specimens V_{2Ref} and V_{2P}.

Specimen	Cracking in the section of				1st Plastic hinge	2nd Plastic hinge	Ultimate load (kN)	Max. displacement D_1 (mm)	Failure mode
	M^{+}_{max} (kN)	M^{-}_{max} (kN)	Int. A (kN)	Int. B (kN)					
V_{2Ref}	180	200	320	280	650	700	753	150	Bending (ductile)
V_{2P}	160	240	180	250	670	720	700	55	Shear slippage (fragile)

6. Conclusions

An experimental work was carried out in order to study the behaviour of concrete-to-concrete interfaces subjected to combination of shear and bending moment and to analyse the application of the design expressions based on the "*shear-friction theory*". The effect of the interface in the shear strength, bending strength and ductility of a beam specimen was also analysed.

Results show that neither the shear strength nor the bending strength of the specimens got affected by the presence of a casting interface. However, the reduced tension strength between the two differently aged concretes, which could be below that of the weakest concrete, lead to a premature cracking along the interface, in the tension zone. This phenomenon was mainly observed in the hogging region where the tension crack occurred firstly along the interface rather than over the support.

The variation of the typical cracking pattern on the web, from diagonal to vertical, pointed to a reduced capacity of the interface to transfer shear loads towards the support, in relation to the reference specimen. This phenomenon did not affect the shear resistance but it was a determining factor in the shear slippage occurred after the formation of a plastic hinge over the continuous support. The crack width increase at the interface led to a deterioration of the mechanisms responsible for the load transfer (aggregate interlock and dowel action), conducting to a shear slippage along the flange in tension and the web, and to the development of a tension crack in the compressed flange. The global bending behaviour of the specimen was similar to the reference model, however with reduced ductility.

The validation of the design expressions to predict the friction strength of the interface when also subjected to a bending moment, and prior to the formation of a plastic hinge, could not be evaluated in these tests, since both V_{1P} and V_{2P} specimens achieved identical ultimate testing loads to those of the reference specimens, and the acting shear forces were always bellow the friction strength predictions. However, the design expressions do not seem adequate, in particular whenever a plastic hinge is likely to develop, as there is no consideration of the friction strength reduction due to width increase of the interface occurred after the yielding of the longitudinal reinforcement, and the consequent limited bending ductility.

As design recommendation, and until better knowledge, it is suggested, if high ductility in bending is required for the interface section, to deviate interfaces between two differently aged concretes to areas where a plastic hinge is unlikely to develop.

Acknowledgements

The authors would like to acknowledge Pavilis – Pré-fabricação S.A.

References

[1] ACI Committee 318. Building code requirements for structural concrete and commentary (ACI 318-14). American Concrete Institute; 2014.
[2] Birkeland PW, Birkeland HW. Connections in precast concrete construction. J Proc 1966;63(3):345–68.
[3] CEN, European Committee for Standardization. EN 1992-1-1, Eurocode 2: design of concrete structures: part 1-1: general rules and rules for buildings, 2004.
[4] Giaccio G, Giovambattista A. Bleeding: evaluation of its effects on concrete behaviour. Mater Struct 1986;19(4):265–71.
[5] Mattock AH, Hawkins NM. Shear transfer in reinforced concrete-recent research. PCI J 1972(17).
[6] Mattock AH, Johal L, Chow H. Shear transfer in reinforced concrete with moment or tension acting across the shear plane. Precast/Prestress Concr Inst J 1975;20(4).
[7] Randl N. Investigations on transfer of forces between old and new concrete at different joint roughness PhD thesis. Austria: University of Innsbruck; 1997.
[8] Randl N. Design recommendations for interface shear transfer in fib Model Code 2010. Struct Concr 2013;14(3):230–41.
[9] Santos PMD, Júlio ENBS. Development of a laser roughness analyser to predict in situ the bond strength of concrete-to-concrete interfaces. Mag Concr Res 2008;60(5):329–37.
[10] Santos PMD, Júlio ENBS. A state-of-the-art review on shear-friction. Eng Struct 2012;45:435–48.
[11] Tassios TP, Vintzēleou EN. Concrete-to-concrete friction. J Struct Eng 1987.
[12] Tsoukantas S, Tassios T. Shear resistance of connections between reinforced concrete linear precast elements. ACI Struct J 1989;86(3).
[13] Vintzēleou E, Tassios T. Mechanisms of load transfer along interfaces in reinforced concrete: prediction of shear force vs. shear displacement curves. Studi ricerche-Corso perfezionamento costruzioni cemento armato Fratelli Pasenti 1985;7:121–61.
[14] Vintzēleou E, Tassios T. Mathematical models for dowel action under monotonic and cyclic conditions. Mag Concr Res 1986;38(134):13–22.
[15] Walraven JC. Fundamental analysis of aggregate interlock. J Struct Div 1981;107(11):2245–70.
[16] Walraven J, Frenay J, Pruijssers A. Influence of concrete strength and load history on the shear friction capacity of concrete members. PCI J 1987;32(1):66–84.
[17] Walraven Bigaj-van et al. Fib model code for concrete structures 2010. Ernst & Sohn, Wiley; 2013.